THE JOURNAL OF PHYSICAL CHEMISTRY A

ARTICLE

pubs.acs.org/JPCA

# Abilities of Different Electron Donors (D) to Engage in a P···D Noncovalent Interaction

Steve Scheiner* and Upendra Adhikari

Department of Chemistry and Biochemistry, Utah State University, Logan, Utah 84322-0300, United States

Supporting Information

**ABSTRACT:** Previous work has documented the ability of the P atom to form a direct attractive noncovalent interaction with a N atom, based in large measure on the charge transfer from the N lone pair into the $\sigma^*$ antibonding orbital of the P−H that is turned away from the N atom. The present work considers whether other atoms, namely, O and S, can also participate as electron donors, and in which bonding environments. Also considered are the $\pi$-systems of multiply bonded C atoms. Unlike an earlier observation that the interaction is unaffected by the nature of the electron-acceptor atom, there is strong sensitivity to the donor. The P···D binding energy diminishes in the order D = $NH_3$ > $H_2CO$ > $H_2CS$ > $H_2O$ > $H_2S$, different from the patterns observed in both H and halogen bonds. The P···D interactions are comparable to, and in some cases stronger than, the analogous H-bonds formed by HOH as proton donor. The carbon $\pi$ systems form surprisingly strong P···D complexes, augmented by the back-donation from the P lone pair to the C−C $\pi^*$ antibond, which surpass the strengths of H-bonds, even some with HF as proton donor.

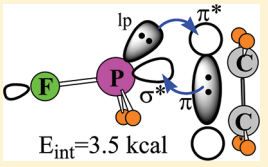


## INTRODUCTION

The importance of noncovalent forces to chemistry and biology cannot be overstated.[1−5] As a prominent and important example, hydrogen bonds have motivated a long history of study,[6−12] which has documented that they derive their strength from a combination of electrostatic with covalent forces.[13−23] While the earliest codification of the H-bond was restricted to electronegative atoms like N and O, the more modern view[20,24−35] has broadened to include C or Cl as proton donor atom, and the accepting unit can contribute electron density via $\pi$ bonds, $\sigma$ bonds, metal atoms, or even another H atom.

Another sort of primary noncovalent interaction, with a shorter history than H-bonds, is the halogen bond wherein the bridging H is replaced by a halogen atom.[36−47] The Coulombic part of the attraction has been attributed to the shape of the electrostatic potential around the halogen atom, which despite an overall negative charge, contains a small positive region that can attract an electronegative partner atom. Yet, like the H-bond, there are important contributions of induction and dispersion forces to halogen bonds as well. The literature also contains instances of other attractive forces between nonhalogen electronegative atoms such as S and O,[48−59] understanding of which continues to grow.

Recent work in this laboratory has identified a fundamentally different sort of noncovalent interaction between a P atom and the N atom on another molecule, with no intervening H or halogen atom.[60] In an illustrative case, the global minimum on the surface of the $PH_3/NH_3$ heterodimer[61] eschews any sort of NH···P or PH···N H-bonding, containing instead a direct interaction between the electronegative P and N atoms. A primary source of the stability of this complex is a certain amount of charge transfer from the N lone pair into the $\sigma^*$ antibond of the P−H bond. But unlike a PH···N H-bond where this same charge transfer might take place, the pertinent H atom is rotated directly away from the N lone pair, so that the charge is transferred into the other lobe of the $\sigma^*$ orbital, on the P end of the P−H bond. In addition to this charge transfer effect, there is also a sizable electrostatic attraction, as well as a dispersion component. Subsequent work[62] has demonstrated that this sort of interaction is not unique to P, but is also characteristic of other second-row atoms S and Cl, as well as the third-row congener As.

With particular regard to P···N, it has very recently been shown[63] that while this interaction between simple hydride $PH_3$ and $NH_3$ molecules is rather weak, less than 2 kcal/mol, it is enhanced if the H atom of the phosphine is replaced by a more electronegative group. For example, even a single Cl, F, or $NO_2$ substituent multiplies the interaction energy as much as 5-fold, to the point where the P···N interaction surpasses the strength of the paradigmatic H-bond in the water dimer. The ability of a substituent to strengthen the attraction has been recently shown[64] to permit even two N atoms to attract one another, as in the case of $FH_2N···NH_3$, which is bound by 4 kcal/mol, comparable to that of the H-bonded water dimer, even though the unsubstituted $NH_3$ dimer will not engage in this sort of N···N interaction. Interestingly, double or triple substitution does not further amplify this interaction,[65] a dramatic difference with H-bonding whose strength continues to grow as more electron-withdrawing substituents are added to the proton donor molecule. Experimental confirmation of these sorts of interactions has arisen from examination[63−65] of a number of crystal structures in the literature. It would thus appear that this particular interaction is an important one, in the same class as

**Received:** August 26, 2011
**Revised:** September 6, 2011
**Published:** September 08, 2011

H and halogen bonds, that warrants a great deal more study and characterization.

All of the previous investigation of this noncovalent force has been concerned with how it is affected by variation of the electron acceptor molecule. The present work shifts attention to the electron donor, which has been modeled only by $NH_3$ to this point. While it might be anticipated that replacement of the N atom with others that are able to donate electrons will affect the interaction, the reader is reminded that, contrary to expectations, an earlier study[62] showed no substantial perturbation caused by replacement of the electron acceptor atom P by S, Cl, or As. To examine this question in detail, the N of the electron donor is replaced by O and S. In addition to their single-bonded models HOH, HSH, and $CH_3OH$, they are also considered in the context of double-bonded valency in $H_2C{=}O$ and $H_2C{=}S$. Another sort of system that is known to donate electrons in H-bonded situations is the $\pi$-electron cloud of hydrocarbons. Also considered in this light then are $HC{\equiv}CH$, $H_2C{=}CH_2$, the conjugated system $H_2C{=}CH{-}CH{=}CH_2$, and the fully aromatic $C_6H_6$.

Each of these molecules is paired with $FH_2P$ as a model electron acceptor molecule. For each pair of molecules, the potential energy is thoroughly searched for all minima, not just that which contains the direct P···D (D = O, S, C) interaction. In this way, any such P···D interaction can be compared directly with other sorts of molecular interactions that might be present, such as H or halogen bonds or simple dipole−dipole attractions. The results show that O is not quite as strong an electron donor as is N, and S is still weaker, but that both O and S are strengthened by involvement in a double C=D bond. The carbon $\pi$ systems are quite proficient electron donors to P, even more so than when participating in OH···$\pi$ H-bonds. The uniqueness of the P···D interaction is underscored by the observation that the effects of different electron donors on the binding strength are quite different than the patterns observed in H and halogen bonds. Perhaps, most surprisingly, the direct P···D interaction is shown to be stronger than a large number of widely occurring H-bonds, even many with OH as proton donor.

## COMPUTATIONAL METHODS

The Gaussian 09 package[66] was applied to all systems. Geometries were optimized at the ab initio MP2/aug-cc-pVDZ level, an approach which has been shown to be of high accuracy, especially for weak intermolecular interactions of the type of interest here[45,67−73] where the data are in close accord with CCSD(T) values with larger basis sets[63,74] and in nearly perfect coincidence with experimental energetics.[75] The potential energy surface of each pair was examined to identify all minima, by using a variety of different starting points for geometry optimizations. Minima were verified as having all real vibrational frequencies. Interaction energies were computed as the difference in energy between the dimer, and the sum of the optimized energies of the isolated monomers, corrected for basis set superposition error by the counterpoise procedure,[76] and by zero-point vibrational energies. Natural bond orbital (NBO) analysis[77,78] was carried out via the procedures contained within Gaussian. The interaction energy was decomposed by the symmetry-adapted perturbation theory (SAPT) procedure,[79,80] implemented via the MOLPRO set of codes,[81] a technique that is subject to less artifact than Kitaura-Morokuma.[82]

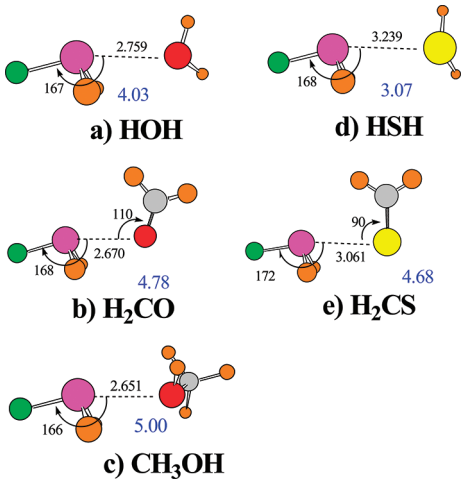


**Figure 1.** Optimized geometries of complexes pairing $FH_2P$ with various electron donor molecules: distances in Å and angles in degs. Counterpoise-corrected binding energy reported as blue number.

**Table 1. Energetic, Geometric, and Electronic Aspects of FP···D Complexes, All with $FH_2P$ as Electron Acceptor**

| | HOH | $H_2CO$ | $CH_3OH$ | HSH | $H_2CS$ | $NH_3$ |
|---|---|---|---|---|---|---|
| $-\Delta E$, kcal/mol | 4.03 | 4.78 | 5.00 | 3.07 | 4.68 | 6.19 |
| R(P···D), Å | 2.759 | 2.670 | 2.651 | 3.239 | 3.061 | 2.624 |
| $\Delta q^a$, me | 11.6 | 17.3 | 19.0 | 17.3 | 33.8 | 33.3 |
| $E(2)$,[b] kcal/mol | 7.69 | 9.70 | 10.91 | 8.44 | 14.85 | 18.18 |
| $\Delta r$(F−P), mÅ | 11.3 | 11.5 | 14.1 | 8.9 | 13.2 | 26.5 |

[a] $D_{lp} \rightarrow \sigma^*(F{-}P)$ charge transfer, summed over both lone pairs of O or S. [b] NBO perturbation energy corresponding to $D_{lp} \rightarrow \sigma^*(F{-}P)$, summed over both lone pairs of O or S.

## RESULTS

**Donors Containing Electronegative Atoms.** The global minima of the dimers pairing $FH_2P$ with HOH, HSH, $H_2CO$, $H_2CS$, and $CH_3OH$ are illustrated in Figure 1. In all cases, the structure can be described as containing a FP···D interaction, in which the P and D atoms approach one another directly, and the F atom stands nearly directly opposite D; these $\theta$(FP···D) angles are all in the narrow range between 167 and 172°. The intermolecular distances for the P···O interactions are also fairly consistent from one complex to another, varying between 2.65 Å for $CH_3OH$ to 2.76 Å for HOH. The R(P···S) distances are a bit longer, consistent with the larger atomic radius of S.

Also displayed in Figure 1 are the interaction energies, corrected for basis set superposition error by the counterpoise procedure. These quantities are also reported in the first line of Table 1 where it may be seen that the change of the single bonds in HOH to the double bond in $H_2CO$ yields an increase in the interaction energy by some 20%; a slightly larger increment occurs upon replacing one of the H atoms of $OH_2$ by a methyl group. These energy changes are mirrored by the contractions of the intermolecular distances reported in the next line of Table 1. Comparison of the aforementioned values with those reported in the next two columns of Table 1 reveals that replacement of O by S reduces the interaction energies. The difference between HOH and HSH of 1 kcal/mol is much larger than the very small difference between $H_2CO$ and $H_2CS$. As a point of comparison,

**Table 2. SAPT Decompositions (kcal/mol) of the Complexation Energies of the FP···D Complexes, All with $FH_2P$ as Partner Molecule**

| | HOH | $H_2CO$ | $CH_3OH$ | HSH | $H_2CS$ | $NH_3$ |
|---|---|---|---|---|---|---|
| ES | −8.38 | −11.16 | −11.54 | −6.72 | −12.43 | −18.21 |
| EX | 8.16 | 12.08 | 13.51 | 8.98 | 16.74 | 22.07 |
| IND | −4.87 | −8.61 | −9.16 | −8.41 | −18.11 | −19.91 |
| IND+EXIND | −1.32 | −1.91 | −2.03 | −1.19 | −2.42 | −4.08 |
| DISP | −3.25 | −4.80 | −5.43 | −3.97 | −6.50 | −6.39 |
| DISP+EXDISP | −2.69 | −3.92 | −4.46 | −3.25 | −5.14 | −4.90 |

data are reported in the last column for the reference $NH_3$ molecule, which may be seen to form a stronger interaction.

As has been described previously,[83] the stability of each of these complexes relies to some extent upon the transfer of electron density from the lone pair of the electron donor to the $\sigma^*$ antibonding orbital of the electron acceptor, in this case $FH_2P$. Some measures of this process are recorded in the next few rows of Table 1. First of these is the amount of density assigned to this particular transfer by the NBO procedure, $\Delta q$, followed by $E(2)$, which refers to the second-order perturbation energy of the same process. Because both O and S contain two lone pairs, the quantities listed in Table 1 represent the sum of the two. The final row contains the stretch of the F−P bond that occurs upon formation of the complex, which is attributed to the extra density that is transferred into its antibonding orbital.

Examination of the data indicates that all of these measures of electron density increase upon going from HOH to $H_2CO$ and then to $CH_3OH$, mirroring the rise in the interaction energy. The switching from O to S as electron donor atom results in a sizable increase in $\Delta q$ and $E(2)$, even though the interaction itself is weakened slightly. The F−P bond stretch, on the other hand, correlates a bit more closely with $\Delta E$, suffering a decline on going from HOH to HSH. The computed data for reference electron donor $NH_3$ presented in the last column of the table are consistent with the stronger nature of the $FH_2P\cdots NH_3$ binding.

To obtain a deeper understanding of the source of the bonding, the total interaction energy of each complex was decomposed into its various constituent parts. The various SAPT components are displayed in Table 2, which shows some strong parallels with the total interaction energies in Table 1. Within the O series, the ES component increases in the order HOH ≪ $H_2CO$ < $CH_3OH$, as does EX, IND, and DISP. These components are considerably larger for $H_2CS$ than for HSH. With regard to their relative magnitudes, the terms follow the order ES > IND > DISP for the O molecules, but the induction energy is larger than ES for the S systems, particularly so for $H_2CS$. The last column pertains to the N electron donor, for which all of the components are larger than those for the O and S systems. The only exception is the large dispersion energy for $H_2CS$ which slightly exceeds that of $NH_3$. A final point concerns the induction energies. These quantities in Table 2 are fairly similar to the $E(2)$ values in Table 1, which reinforces the notion that it is the $D_{lp} \rightarrow \sigma^*(PF)$ transfer, which accounts for a large portion of the full induction energy. Of course these quantities are not exactly the same, notably for HOH and $H_2CS$, which reminds us that the full induction energy does contain a number of other terms.

The NBO data reported in Table 1 refer explicitly to the transfer of density between certain pairs of orbitals, specifically from the lone pair of the electron donor atom to the F−P $\sigma^*$ antibond. There are of course a wide array of other shifts that are taking place, including those internal to each molecule. The combined effect of all of these shifts are visualized in Figure 2 which represents increases in density by blue contours and decreases by red. Along with the systems considered here, the $FH_2P\cdots NH_3$ prototype system is included in Figure 2f for purposes of comparison. Inspection reveals a commonality of patterns in all cases. Focus is drawn to the P···D axis, where density is lost immediately to the right of the P atom, and gained to the left of the D atom, whether O, S, or N. There is some gain observed also on both sides of the F atom, as well as around the circumference of P, perpendicular to the P···D axis. Density is drained from the area to the immediate right of D, balancing the gain to its left. This pattern of electron redistribution may be taken as a fingerprint of sorts of this type of P···D interaction.

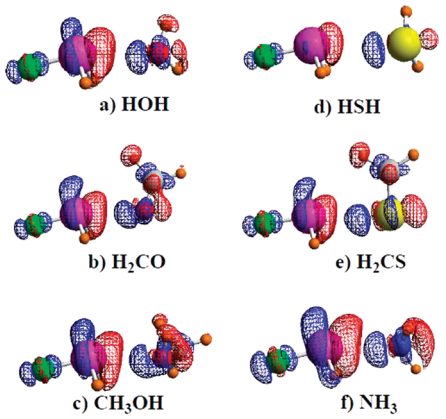


**Figure 2.** Density shifts occurring in the indicated $FH_2P\cdots D$ complexes upon formation of each complex. Blue regions indicate a density increase, red a density decrease. Contours are shown at the 0.001 au level.

As noted before,[83] it is not entirely surprising that the full density shifts in Figure 2 do not affirm the NBO data, as the latter refer to a specific pair of orbitals, and the former to the entire basis set. The charge shifts occurring from one molecule to the other, emphasized by the NBO treatment, are combined with polarizations internal to each molecule in Figure 2. It is for this same reason that total electron density rearrangements monitored in H-bonds[11,84−89] are at odds with the $n \rightarrow \sigma^*$ transfer that is a well-known characteristic of H-bonds. This idea has been confirmed recently[90] by calculations that divided the electron redistributions that occur upon formation of a H-bonded dimer into two separate contributions. The shifts that are attributed to the transfer of total density from one monomer to the other clearly show the loss of density from the lone pair of the proton acceptor atom, and the gain in the $\sigma^*$ region of the covalent O−H bond of the proton donor, verifying the predictions of a score of NBO analyses of numerous H-bonds. On the other hand, the pattern that results directly from polarization effects is just the opposite, but larger in magnitude. In other words, the loss of density in the proton acceptor lone pair due to a very real $n \rightarrow \sigma^*$ charge transfer is masked by a larger density increase in this same region associated with intramolecular density rearrangements. The combination of these two effects into a single map of charge density shift thus shows the familiar increase of density in the lone pair area.

The SAPT analysis had indicated a large fraction of the interaction energy is associated with the electrostatic interaction.

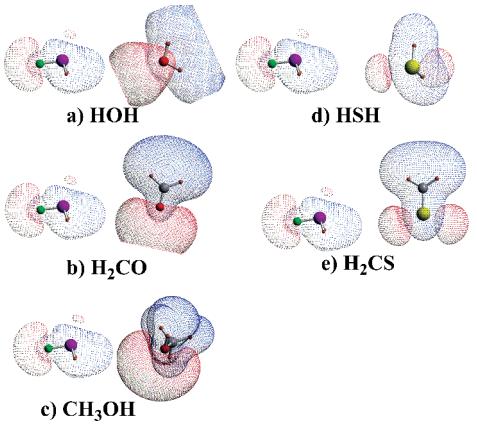


**Figure 3.** Electrostatic potentials of isolated monomers, oriented as they are within the optimized complexes with $FH_2P$. Blue and red regions indicate positive and negative potentials, respectively; contours at the ±0.02 au level.

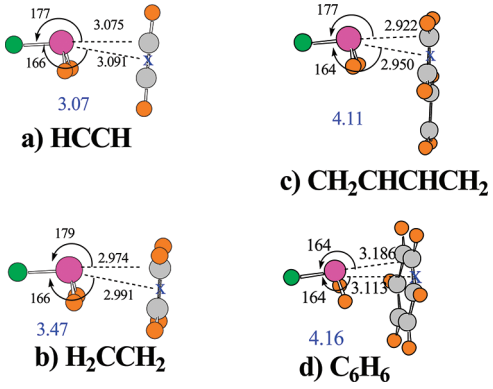


**Figure 4.** Optimized geometries of complexes pairing $FH_2P$ with each of several unsaturated C-containing molecules. Distances in Å and angles in degs. Blue X represents center of indicated C−C bond. Counterpoise-corrected binding energy reported as blue number.

In order to achieve a better understanding of this component, the electrostatic potential of each monomer was computed, and these potentials superimposed upon each other as occurs in the equilibrium geometry of each dimer. These potentials are exhibited in Figure 3 where it may be seen that the positive (blue) region to the right of P of $FH_2P$ approaches a negative (red) region of each electron donor molecule. Clearly, then, the electrostatic interaction is a favorable one. On the other hand, this potential is not sufficient to explain the equilibrium orientations of the various complexes. Specifically, in the cases of the three O-donors on the left side of Figure 3, a clockwise rotation of the right-hand molecule would better align its red region with the blue potential on the left. In other words, electrostatic considerations alone would lead to a larger $\theta$(P···OX) angle (X = C, H) than is observed. It is likely that the need to align one of the O lone pairs with the P−F $\sigma^*$ antibond accounts for the more acute angle. In the S cases, the electrostatic potentials of the HSH and $H_2CS$ monomers more closely resemble the directions of the two S lone pairs, so the electrostatic and $n \rightarrow \sigma^*$ transfers have the same requirements, and no such conflict arises.

**Carbon-Containing Electron Donors.** The $\pi$ systems of the various unsaturated hydrocarbon molecules can also serve as electron donors. The global minimum of the potential energy surface of $FH_2P$ with HC≡CH, $H_2C{=}CH_2$, 1,3-butadiene, and benzene are all illustrated in Figure 4 where it may be seen that once again, the P−F bond is swung around away from the source of electrons. The binding energies of these complexes are all within the 3−4 kcal/mol regime. The triply bonded HC≡CH is the most weakly bound, followed by $H_2C{=}CH_2$, and then by the two conjugated systems. The full aromaticity of benzene does not appear to add significantly to the energetics of the conjugated $C_4H_6$. These binding energies are comparable to, albeit a bit smaller than, those reported in Table 1 for the electronegative electron donors. The P atom is located above the midpoint of the C−C bond, but is skewed slightly toward one C atom over the other. (The blue X in each diagram indicates this bond center.) As in the systems described earlier, the intermolecular distance diminishes as the interaction energy climbs, with the exception of the fully aromatic $C_6H_6$ complex.

**Table 3. Energetic, Geometric, and Electronic Aspects of FP···D Complexes, for Carbon-Containing Donors, All with $FH_2P$ as Partner Molecule**

| | HCCH | $H_2CCH_2$ | $CH_2CHCHCH_2$ | $C_6H_6$ |
|---|---|---|---|---|
| $-\Delta E$, kcal/mol | 3.04 | 3.47 | 4.11 | 4.16 |
| $R$(P···C), Å | 3.075 | 2.974 | 2.922 | 3.186 |
| $\Delta q_{FP}$[a], me | 10.9 | 18.9 | 18.8 | 31.3 |
| $E(2)_{FP}$[a], kcal/mol | 5.06 | 8.01 | 8.02 | 7.68 |
| $\Delta q_{CC}$[b], me | 3.8 | 7.1 | 7.6 | [c] |
| $E(2)_{CC}$[b], kcal/mol | 2.07 | 3.52 | 3.58 | [c] |
| $\Delta r$(F−P), mÅ | 6.2 | 9.2 | 11.0 | 8.1 |
| $\Delta r$(C−C), mÅ | 1.8 | 3.8 | 5.2 | 2.0 |

[a] $\pi$(C−C) → $\sigma^*$(F−P). [b] $P_{lp} \rightarrow \pi^*$(CC) charge transfer. [c] NBO treatment suffers partial breakdown with $C_6H_6$.

The other important properties of these complexes are displayed in Table 3. Switching out the molecules of Figure 1 by the C-containing partner molecules eliminates the lone pair as electron donor. Instead, the electron density is acquired from the $\pi$ system. The NBO parameters of the charge transfer from the C−C $\pi$ bond to the F−P $\sigma^*$ antibond are reported in Table 3 as $\Delta q_{FP}$ and $E(2)_{FP}$. Like the binding energies, the values of $E(2)$ are slightly smaller than those in Table 1. The magnitudes of the charge transferred, $\Delta q_{FP}$, however, are in the same range as those for the electronegative atoms.

The carbon $\pi$ systems add a new factor to the binding of these complexes. The presence of a low-lying C−C $\pi^*$ orbital permits electron transfer into it from the P lone pair. As may be seen by the relevant measures of this shift, $\Delta q_{CC}$ and $E(2)_{CC}$, this phenomenon is quite significant, amounting to 35−45% of the dominant $D_{lp} \rightarrow \sigma^*$(PF) quantities.

As in the earlier cases, the accumulation of electron density in the antibonding P−F region elongates this bond, by between 6 and 11 me, again slightly smaller than the stretches reported in Table 1. The second, and new, factor in the C systems, whereby density is added to the C−C $\pi^*$ system, stretches this bond as well, by amounts listed in the last row of Table 3.

There are several interesting observations about the data reported above. In the first place, the single C=C $\pi$ bond in ethylene makes for a slightly stronger interaction with $FH_2P$, than does the pair of such $\pi$ bonds in HC≡CH. One may interpret this distinction as a tentative rule that $sp^2$ hybridization is superior to sp in such interactions. The addition of a second

**Table 4. SAPT Decompositions (kcal/mol) of the Complexation Energies of the FP···D Complexes, All with $FH_2P$ as Partner Molecule**

| | HCCH | $H_2CCH_2$ | $CH_2CHCHCH_2$ | $C_6H_6$ |
|---|---|---|---|---|
| ES | −6.94 | −9.62 | −10.61 | −6.75 |
| EX | 9.71 | 15.03 | 17.75 | 11.73 |
| IND | −7.77 | −14.43 | −16.65 | −7.46 |
| IND + EXIND | −1.13 | −1.78 | −2.12 | −1.17 |
| DISP | −4.68 | −6.54 | −8.17 | −7.60 |
| DISP + EXDISP | −3.83 | −5.23 | −6.61 | −6.36 |

C═C bond in butadiene which can conjugate with the first adds to the interaction although nothing further arises from the full aromaticity of benzene. In fact, the two molecules lie a bit further apart in the latter case. It might be noted also that the P atom prefers a position directly above one C═C bond, as opposed to a central location above the middle of the $C_6H_6$ molecule.

The SAPT components of the interactions reported in Table 4 show that each of the elements climb in magnitude from HCCH to $H_2C═CH_2$, and then to butadiene, pretty much parallel to the rise in the total interaction energy. The benzene terms, in contrast, are surprisingly small, contrasting with the stronger total interaction of this electron donor. It is likely that these smaller terms are due at least in part to the longer intermolecular separation in the $FH_2P···C_6H_6$ complex. Note, however, that the dispersion energy in this complex is rather large, which might be attributed to the high polarizability of the aromatic $\pi$ system of benzene.

It is interesting to compare the individual energy components in Table 4 with those of the more electronegative donors of Table 2. Taking butadiene as a system that has the largest such quantities as one end of the spectrum, its ES, EX, and IND components are all comparable to those in Table 2. The dispersion energy is particularly large for butadiene, greater than the same quantity for any donor of Table 2, even those molecules with much stronger total binding strength. Indeed, one distinguishing feature of all the C-containing systems is a disproportionately large contribution from DISP. The latter component is in fact the single largest contributor to the $FH_2P···C_6H_6$ dimer.

The shifts in total electron density accompanying the formation of the complexes of $FH_2P$ with the C systems are illustrated in Figure 5. Comparison with those in Figure 2 indicates strong similarities. Once again, the strongest loss is observed to the immediate right of the P atom, and a gain further to its right. In this case, the increment occurs in the region between the two C atoms, to the left of the C−C bond, rather than to the left of a single (O, S, or N) atom. Also in common, accumulations of density occur along the F−P axis. Just as the C-containing systems are somewhat more weakly bound than those in Figure 2, the patterns in Figure 5 are also slightly attenuated. And again there is the tendency of more strongly bound complexes within this C subset to manifest larger density shifts. These charge shift patterns, then, suggest strong similarities whether the electron-donating entity is a C−C $\pi$ bond or an electronegative atom like O, S, or N.

A final remaining question concerns whether electrostatic considerations in the C-systems represent a strong influence in the orientation adopted by the two subunits in the global minimum. The electrostatic potentials of the relevant systems are placed in juxtaposition in Figure 6. It is immediately obvious

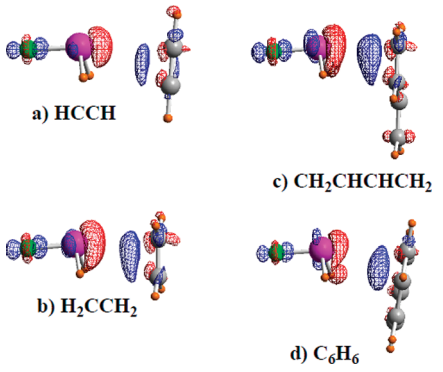


**Figure 5.** Density shifts occurring in the indicated $FH_2P···D$ structures upon formation of each complex. Blue regions indicate a density increase, red a decrease. Contours are shown at the 0.001 au level.

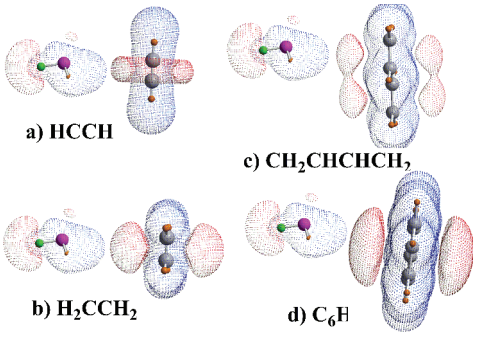


**Figure 6.** Electrostatic potentials of isolated monomers, oriented as they are within the optimized complexes with $FH_2P$. Blue and red regions indicate positive and negative potentials, respectively; contours at the ±0.02 au level.

that there is a strong overlap between the positive region to the right of the P atom and a negative area that lies directly above the midpoint of the C−C multiple bonds. Note that the aforementioned negative potential is most prominent above the double bonds of butadiene in Figure 6c, so that electrostatic considerations reinforce the charge transfer effect arising from optimal overlap of the appropriate $\pi$ orbital with the P−F $\sigma^*$ antibond. The case of benzene is a bit different in that the maximum of its negative density lies directly above the center of the molecule. Nonetheless, the approaching $FH_2P$ molecule forgoes this position for one closer to an individual C−C bond. This latter preference is likely due the fact that whereas the ES potential is most negative above the molecular center, the electron density is larger above the individual C−C bonds. This off-center geometry thus permits a better overlap between the relevant orbitals of the two molecules that engage in $\pi(CC) \rightarrow \sigma^*(PF)$ and $P_{lp} \rightarrow \pi^*(CC)$ charge transfers.

**Secondary Minima.** As indicated above, all of the structures presented to this point represent the global minimum in the potential energy surface of each heterodimer. Examination of secondary minima provides useful insights into the comparative strengths of the FP···D interactions with H-bonds or other noncovalent forces. (All of these secondary minima are presented graphically in the Supporting Information, along with their energies and important interatomic distances.) The $FH_2P/OH_2$ heterodimer contains only one secondary minimum, characterized as a cyclic structure containing a pair of H-bonds. The

primary interaction is a OH···F H-bond, with $R$(H···F) = 2.02 Å, complemented by a much longer PH···O interaction ($R$ = 2.71 Å). Despite the presence of these two H-bonds, this complex is less strongly bound than the primary minimum by 1 kcal/mol. There are two secondary minima when $H_2O$ is replaced by $H_2S$. Again, both of these contain a pair of H-bonds (SH···F and SH···P), and again, they are both less stable than the FP···S structure by 1 kcal/mol.

The double-bonded $H_2CX$ (X = O, S) molecules present a few more secondary minima. The most stable of these contains both a CH···F and PH···X H-bond. Whether O or S, the CH···F bond is the shorter of the two, at 2.4 Å. Another minimum, very similar in energy, also contains this same pair of H-bonds, except that the PH approaches the O/S atom from above the plane of the $H_2CX$ molecule, rather than from within its plane as in the former case. The third and least stable of the $H_2CO$ minima is stabilized by a bifurcated pair of CH···F H-bonds. This same structure is present also for X = S, but is complemented by two other minima, even less stable. One of them also sports a bifurcated CH···F pair, and the least stable of all contains what appears to be a bifurcated PH···S pair, although the two $R$(H···S) distances are rather long at 3.3 Å.

The relative complexity of the $CH_3OH$ molecule leads to 11 minima in addition to the global structure. The most stable quartet of this set all have in common a OH···F H-bond, with $R$(H···F) in the 2.0−2.2 Å range, complemented by a much longer (2.7−3.0 Å) PH···O interaction. These four have similar energies, all 2 kcal/mol less stable than the global minimum. Another geometry is stabilized by a OH···F H-bond without benefit of PH···N interactions so is somewhat higher in energy. Two other complexes contain a bifurcated pair of CH···F H-bonds, one with and one without an auxiliary OH···P interaction. A PH···O interaction occurs along with a CH···F in another structure. The next two minima both contain a single stabilizing interaction, OH···P in one and CH···F in the other. The least stable of the minima on this surface, only 0.4 kcal/mol more stable than the isolated monomers, is most interesting in some sense. While there are no H-bonds of any sort, the FP···C alignment is reminiscent of the global minimum, with the O replaced by the methyl C atom. And indeed, NBO analysis reveals a charge transfer from a methyl C−H bond to the P−F $\sigma^*$ antibond, with $E(2)$ = 0.89 kcal/mol. This transfer is complemented by another ($E(2)$ = 0.50 kcal/mol) from the P lone pair to the C−O $\sigma^*$ antibond, enabled by the proper alignment of the C−O bond.

In summary, the FP···D interaction is clearly the dominant one in these dimers. Its binding energy surpasses those of a wide range of different sorts of H-bonds that occur in the secondary minima, including OH···F, PH···O, CH···F, and OH···P. This greater binding strength is notable first in that the F substituent on the P atom is expected to strengthen the proton-donating power of the phosphine. Second, the single FP···D interaction must compete with other structures which contain not one but two or more H-bonds.

Turning next to the C-containing species, alternate minima contain weak H-bonds. The fairly high acidity of the sp-hybridized CH group of HC≡CH results in a CH···F H-bond which amounts to 1.9 kcal/mol, weaker than the FP···$\pi$ interaction of the global minimum by 1.1 kcal/mol. Still weaker is a CH···P H-bond. The $sp^2$ hybridization of $C_2H_4$ yields a weaker CH proton donor. The two secondary minima on the surface both contain a pair of CH···F H-bonds to the single F atom. In the more stable of the two, the participating H atoms are on different C atoms while they are bound to the same C in the highest energy structure. Like $CH_3OH$, the butadiene molecule also is associated with a number of different secondary minima, nine in this case. Two of these are much like the global minimum of Figure 3, containing a FP···$\pi$ interaction, except that the $FH_2P$ molecule is rotated a bit. The next group of three minima rotates $FH_2P$ so that one of its two H atoms is oriented away from the C−C $\pi$ bond, instead of the F. These structures are about 1.5 kcal/mol less stable than the FP···$\pi$ structure. The remaining minima each contain a pair of CH···F H-bonds, usually fairly long in the range between 2.6 and 2.8 Å. One of the two alternate minima of the complexes with benzene is nearly identical to the global minimum, containing the same FP···$\pi$ interaction, with only slight differences in orientation, but essentially identical in energy. The other minimum is 1 kcal/mol higher and has the $FH_2P$ molecule oriented in such a way that a P−H bond is turned toward the benzene $\pi$ system, in what is primarily a PH···$\pi$ interaction. It is clear then that the FP···$\pi$ interaction is favored in all cases, being more stable than HP···$\pi$, PH···$\pi$, or CH···F H-bonds, even when there are two of the latter.

**Table 5. FP···D Binding Energies (kcal/mol) with $FH_2P$ Compared with H-Bonds Formed with FH and HOH**

| | $FH_2P$ | FH | HOH |
|---|---|---|---|
| $NH_3$ | 6.19 | 11.64 | 5.81 |
| HOH | 4.03 | 7.86 | 4.43 |
| $H_2CO$ | 4.78 | 7.43 | 4.73 |
| $CH_3OH$ | 5.00 | 8.93 | 5.05 |
| HSH | 3.07 | 4.54 | 2.55 |
| $H_2CS$ | 4.68 | 5.52 | 3.84 |
| HCCH | 3.04 | 3.72 | 2.05 |
| $H_2CCH_2$ | 3.47 | 4.08 | 2.27 |
| $C_4H_6$ | 4.11 | 4.06 | 2.68 |
| $C_6H_6$ | 4.16 | 3.92 | 2.88 |

## DISCUSSION AND CONCLUSIONS

Some of these FP···D interactions might be considered surprisingly strong. For example, the water molecule forms an interaction with $FH_2P$ that is very nearly as strong as that with another water. That is, the 4.03 kcal/mol binding energy of $FH_2P$···$OH_2$ is within only 0.4 kcal/mol of the strength of the prototypical H-bond in the water dimer, computed at the same level of theory. To further explore this comparison between FP···D and H-bonding the various electron donors in Figures 1 and 4 were paired with HF and HOH. These two molecules represent powerful proton donors in the H-bonds in which they participate, in particular HF which forms some of the strongest H-bonds known.

The binding energies of all complexes are collected in Table 5, which illustrates some interesting points. In terms of the electron donors in the first six rows that contain electronegative atoms, formation of a H-bond with FH is substantially preferred over a FP···D interaction. This margin of difference is smallest for S donors but is present nonetheless. There is also a preference for the CC $\pi$ bonds of acetylene and ethylene to interact with HF over $FH_2P$. However, this order reverses for the more extended $\pi$ systems of 1,3-butadiene and benzene, where there is a slight preference for the FP···$\pi$ bond over FH···$\pi$. HOH is a

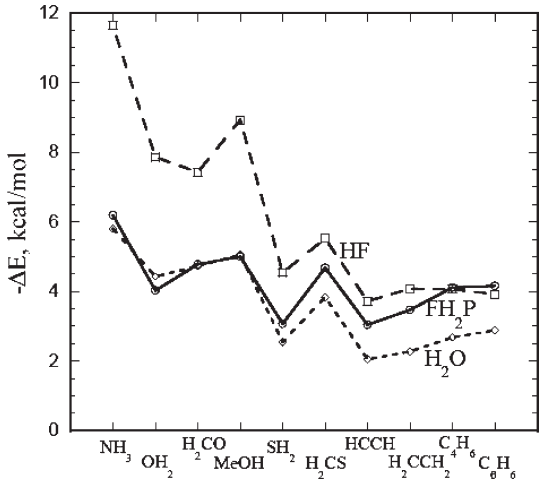


**Figure 7.** Interaction energies of each of the complexes formed by HF, $H_2O$, and $FH_2P$ with various electron donors. Broken lines refer to H-bonds and solid to P···D.

somewhat weaker proton donor than is HF, so the binding energies in the last column of Table 5 are uniformly smaller than those in the preceding column. Indeed, the OH···D H-bonds formed by water are similar to, and usually smaller than, the FP···D binding energies in the first column.

Visualization of these data in Figure 7 exhibits some important patterns. There is some generality in that $NH_3$ forms the strongest complexes, followed by the O-containing electron donors, and then the S analogues. There are discrepancies as well. For example, $H_2CO$ forms a weaker complex with HF than does $OH_2$, but the reverse is true for HOH and $FH_2P$; $H_2CS$ engages more strongly with all three electron acceptors than does $SH_2$. Whereas HF is a uniformly stronger electron acceptor, $FH_2P$ and $OH_2$ are fairly similar to one another, although $FH_2P$ emerges as superior for S-donors. Within the subset of C-donors, the binding energy climbs in the sequence HC≡CH < $H_2C$═$CH_2$ < butadiene < benzene. Perhaps most interesting is the strength of the complexes of $FH_2P$ with the C-donors. The P···$\pi$ interaction is substantially stronger than OH···$\pi$ for all four carbon donors and is even competitive with FH···$\pi$. In fact, a recent calculation[91] enhanced the proton donating power of HOH by replacing one H atom by a halogen (X = F, Cl, Br, or I). Even with this boost, the XOH···$C_6H_6$ H-bonding energy remained lower than the value computed here for $FH_2P$···$C_6H_6$ for all halogen atoms save I.

One may conclude that the FP···D interaction is competitive with even some of the strongest H-bonds. $FH_2P$ is superior to HOH as an electron acceptor from $\pi$ bonds, and can even surpass HF for conjugated systems. The FP···D interaction is as strong as OH···D for electronegative donors and is, in fact, better for S-containing systems. Only the very powerful HF proton donor surpasses $FH_2P$ as electron acceptor, but even that distinction evaporates for C-donors. Comparison of the geometries of the global minimum in each case with secondary minima also demonstrates the superiority of the FP···D interaction over various other sorts of H-bonds such as OH···F, PH···O, CH···F, CH···P, OH···P, or PH···$\pi$. Electron donors are not limited to only very electronegative atoms. In addition to the C atoms examined here, even P can act in this capacity[61] so as to form a P···P interaction. Indeed, the binding energy of such a P···P complex can exceed 4 kcal/mol with certain substituents.[92]

A major component of the P···D binding arises from the charge transfer from the lone pair(s) of the donor atom into the $\sigma^*$ antibond of the P−F bond that lies opposite the donor atom. This transfer is disproportionately larger for second-row S than for O and N, presumably due to the greater polarizability of S compounds. The latter property is also responsible for the large contribution of induction energy for S, greater than ES or DISP, whereas ES represents the greatest contributor for O and N. When the electron donation occurs from a C $\pi$ system, there is a tendency of the P atom to hover immediately above the midpoint of one particular C═C bond, rather than locating itself above the center of the entire molecule. In addition to the $\pi \rightarrow \sigma^*$ transfer, there is a back transfer from the P lone pair into a C−C $\pi^*$ antibond. This second factor may account for the unexpected strength of the P···$\pi$ binding energies. The largest contribution to the interaction is made in three of these four cases by the induction energy, followed by ES and DISP. The exception occurs for the benzene donor in which the dispersion energy is largest, and the electrostatic term the smallest. Consideration of the three-dimensional disposition of the electrostatic potentials of each monomer is consistent with the equilibrium geometries but not fully predictive, as the alignment of the donor lone pair, or C═C density maximum, with the acceptor $\sigma^*$ orbital is another important issue

The concept of a stabilizing charge transfer from a lone pair of one molecule to a $\sigma^*$ antibond of another has strong precedent and is a foundation of some other noncovalent interactions. It has been invoked, for example, to help explain H and halogen bonding[93−96] and has been applied also to chalcogen atoms such as O and S.[48,50,51,53,59,97−101] Its participation in the P···D interactions here should thus not be entirely surprising. Adding to this primary $D_{lp} \rightarrow \sigma^*(PF)$ effect is the back transfer that occurs when the P atom interacts with the carbon $\pi$ systems. It is likely that this auxiliary $P_{lp} \rightarrow \pi^*(CC)$ charge transfer is at least partially responsible for the large interaction energies in these complexes, as compared to the analogous H-bonded complexes in Figure 7. This idea of transfer to $\pi^*$ antibonds is not without precedent either. A similar sort of phenomenon has been invoked[55,56,102] to explain certain close contacts between carbonyl groups in proteins, which has been attributed to a purported transfer of charge from an O lone pair of one subunit to the C═O $\pi^*$ antibonding orbital of the other.

Summarizing the potency of the various electron donors for participation in a P···D bond, N is stronger than O, which is in turn a better donor than is S. The double-bonded O and S atoms in $H_2C$═D are superior to the single bonded HDH analogues; replacement of a H atom by a methyl group enhances the electron-donating ability. The $\pi$ systems of multiply bonded C atoms form surprisingly strong P···$\pi$ bonds, notably superior to OH···$\pi$ interactions and even comparable to FH···$\pi$. These P···$\pi$ interactions are better for CC double than for triple bonds, particularly if the double bond is part of a conjugated $\pi$ system. Indeed, the P···benzene binding is essentially equivalent to the standard OH···O H-bond in the water dimer.

It is reiterated finally that the P···D interaction studied here is fundamentally distinct from both halogen and H-bonds in a number of important ways. Some of the differences have been discussed previously[61−63,65,83] and include the patterns of charge density shift, energy component magnitudes, internal geometry perturbations, sensitivity to angular distortion, dependence upon

identity of electron-accepting atom, and the effect of multiple halogenation. Another distinction arises from the work presented here, concerning the way in which the binding energy varies with the particular electron donor molecule. These differences with H-bonds are exhibited in Figure 7. While these differences are not overly dramatic, comparison with halogen bonds leads to more striking contrasts. It was found previously[103] that halogen bonds weaken as the donor is changed in the order: $H_2CS > H_2CO > NH_3 > H_2S > H_2O$. This pattern is quite different for P···D interactions which, as illustrated in Table 5, is $NH_3 > H_2CO > H_2CS > H_2O > H_2S$. There is some similarity as well. Halogen bonds to the $\pi$-clouds of C-containing systems, like the P···$\pi$ interactions considered here, are also stronger for doubly bonded $H_2C{=}CH_2$, as compared to the triple bond in HC≡CH.[73]

One might expect that the much greater electronegativity of F as compared to P would lead to a P−F $\sigma^*$ antibonding orbital that is biased heavily toward the P. However, NBO evaluation of this orbital indicates a surprising lack of such bias; the shape of this orbital is very little affected by the electronegativity of the group bonded to P, whether F, H, OH, or $CF_3$.[63]

There are a number of chemical situations where such interactions may be important. Phosphines are a common ligand in inorganic systems,[104−106] which typically interacts with nearby groups in the solid state. As one example, a synthetic catalyst has recently been developed which can produce molecular $H_2$ at an unprecedented rate.[107] The efficiency of this catalyst relies upon a pair of pendant seven-membered cyclic diphosphine amine ligands. Interactions of these two ligands with each other, or those between separate catalyst molecules might take advantage of the sort of P···N interactions under consideration here. In the context of biological situations, the electron donor groups considered here are all representative of functional groups within proteins. HSH, for example, is a model of the Cys residue, $CH_3OH$ of hydroxyl groups in Ser or Thr, and benzene approximates the functional group of Phe. The P atom of the phosphate group is bonded to four very electronegative O atoms, so would be unlikely to interact in the fashion indicated. However, trivalent phosphines are a common structural and enzymatic element and their interaction with other molecular units might be controlled by the forces that are the subject of this work.

## ■ ASSOCIATED CONTENT

**Supporting Information.** Graphical representations of all secondary minima. This material is available free of charge via the Internet at http://pubs.acs.org.

## ■ AUTHOR INFORMATION

### Corresponding Author

*E-mail: steve.scheiner@usu.edu.

## ■ REFERENCES

(1) Hobza, P.; Zahradnik, R. *Weak Intermolecular Interactions in Chemistry and Biology*; Elsevier Scientific: Amsterdam, 1980.

(2) Kaplan, I. G. *Theory of Molecular Interactions*; Elsevier: Amsterdam, 1986.

(3) Müller-Dethlefs, K.; Hobza, P. *Chem. Rev.* **2000**, *100*, 143.

(4) Stone, A. J. *The Theory of Intermolecular Forces*; Oxford University Press: Oxford, 2002.

(5) Hobza, P.; Muller-Dethlefs, K. *Non-Covalent Interactions*; RSC: Cambridge, 2010.

(6) Pimentel, G. C.; McClellan, A. L. *The Hydrogen Bond*; Freeman: San Francisco, 1960.

(7) *The Hydrogen Bond. Recent Developments in Theory and Experiments*; Schuster, P., Zundel, G., Sandorfy, C., Eds.; North-Holland Publishing Co.: Amsterdam, 1976.

(8) Hadzi, D.; Bratos, S. Vibrational Spectroscopy of the Hydrogen Bond. In *The Hydrogen Bond. Recent Developments in Theory and Experiments*; Schuster, P., Zundel, G., Sandorfy, C., Eds.; North-Holland Publishing Co.: Amsterdam, 1976; Vol. 2; p 565.

(9) Schuster, P. *Hydrogen Bonds*; Springer-Verlag: Berlin, 1984; Vol. 120.

(10) Jeffrey, G. A.; Saenger, W. *Hydrogen Bonding in Biological Structures*; Springer-Verlag: Berlin, 1991.

(11) Scheiner, S. *Hydrogen Bonding. A Theoretical Perspective*; Oxford University Press: New York, 1997.

(12) Gilli, G.; Gilli, P. *The Nature of the Hydrogen Bond*; Oxford University Press: Oxford, U.K., 2009.

(13) Wieczorek, R.; Dannenberg, J. J. *J. Am. Chem. Soc.* **2003**, *125*, 8124.

(14) Alabugin, I. V.; Manoharan, M.; Peabody, S.; Weinhold, F. *J. Am. Chem. Soc.* **2003**, *125*, 5973.

(15) Hernández-Soto, H.; Weinhold, F.; Francisco, J. S. *J. Chem. Phys.* **2007**, *127*, 164102.

(16) Li, Q.; Liu, H.; An, X.; Gong, B.; Cheng, J. *J. Mol. Struct.: THEOCHEM* **2008**, *861*, 14.

(17) Bhate, M. P.; Woodard, J. C.; Mehta, M. A. *J. Am. Chem. Soc.* **2009**, *131*, 9579.

(18) Samanta, A. K.; Pandey, P.; Bandyopadhyay, B.; Chakraborty, T. *J. Phys. Chem. A* **2010**, *114*, 1650–1656.

(19) Wang, W.; Zhang, Y.; Ji, B. *J. Phys. Chem. A* **2010**, *114*, 7257–7260.

(20) Alkorta, I.; Elguero, J.; Bene, J. E. D. *Chem. Phys. Lett.* **2010**, *489*, 159.

(21) Bene, J. E. D.; Alkorta, I.; Elguero, J. *Phys. Chem. Chem. Phys.* **2011**, *13*, 13951.

(22) Thakur, T. S.; Kirchner, M. T.; Bläser, D.; Boese, R.; Desiraju, G. R. *Phys. Chem. Chem. Phys.* **2011**, *13*, 14076.

(23) McDowell, S. A. C.; Buckingham, A. D. *Phys. Chem. Chem. Phys.* **2011**, *13*, 14097.

(24) Desiraju, G. R.; Steiner, T. *The Weak Hydrogen Bond in Structural Chemistry and Biology*; Oxford: New York, 1999.

(25) Scheiner, S.; Gu, Y.; Kar, T. *J. Mol. Struct.: THEOCHEM* **2000**, *500*, 441.

(26) Gu, Y.; Kar, T.; Scheiner, S. *J. Mol. Struct.* **2000**, *552*, 17.

(27) *Hydrogen Bonding—New Insights*; Grabowski, S. J., Ed.; Springer: Dordrecht, 2006.

(28) Orlova, G.; Scheiner, S. *J. Phys. Chem. A* **1998**, *102*, 4813.

(29) Desiraju, G. R. *Angew. Chem., Int. Ed.* **2011**, *50*, 52.

(30) Arunan, E.; Desiraju, G. R.; Klein, R. A.; Sadlej, J.; Scheiner, S.; Alkorta, I.; Clary, D. C.; Crabtree, R. H.; Dannenberg, J. J.; Hobza, P.; Kjaergaard, H. G.; Legon, A. C.; Mennucci, B.; Nesbitt, D. J. *Pure Appl. Chem.* **2011**, *83*, 1637.

(31) Vaz, P. D.; Nolasco, M. M.; Gil, F. P. S. C.; Ribeiro-Claro, P. J. A.; Tomkinson, J. *Chem.—Eur. J.* **2010**, *16*, 9010.

(32) Veken, B. J. v. d.; Delanoye, S. N.; Michielsen, B.; Herrebout, W. A. *J. Mol. Struct.* **2010**, *976*, 97.

(33) Takahashi, O.; Kohno, Y.; Nishio, M. *Chem. Rev.* **2010**, *110*, 6049.

(34) Rizzato, S.; Bergès, J.; Mason, S. A.; Albinati, A.; Kozelka, J. *Angew. Chem., Int. Ed.* **2010**, *49*, 7440.

(35) Falvello, L. R. *Angew. Chem., Int. Ed.* **2010**, *49*, 10045.

(36) Lommerse, J. P. M.; Stone, A. J.; Taylor, R.; Allen, F. H. *J. Am. Chem. Soc.* **1996**, *118*, 3108.

(37) Alkorta, I.; Rozas, s.; Elguero, J. *J. Phys. Chem. A* **1998**, *102*, 9278.

(38) Wash, P. L.; Ma, S.; Obst, U.; Rebek, J. *J. Am. Chem. Soc.* **1999**, *121*, 7973.

(39) Glaser, R.; Chen, N.; Wu, H.; Knotts, N.; Kaupp, M. *J. Am. Chem. Soc.* **2004**, *126*, 4412.

(40) Nguyen, H. L.; Horton, P. N.; Hursthouse, M. B.; Legon, A. C.; Bruce, D. W. *J. Am. Chem. Soc.* **2004**, *126*, 16.
(41) Caronna, T.; Liantonio, R.; Logothetis, T. A.; Metrangolo, P.; Pilati, T.; Resnati, G. *J. Am. Chem. Soc.* **2004**, *126*, 4500.
(42) Cavallo, G.; Metrangolo, P.; Pilati, T.; Resnati, G.; Sansotera, M.; Terraneo, G. *Chem. Soc. Rev.* **2010**, *39*, 3772.
(43) Sarwar, M. G.; Dragisic, B.; Salsberg, L. J.; Gouliaras, C.; Taylor, M. S. *J. Am. Chem. Soc.* **2010**, *132*, 1646.
(44) Politzer, P.; Murray, J. S.; Clark, T. *Phys. Chem. Chem. Phys.* **2010**, *12*, 7748.
(45) Chudzinski, M. G.; McClary, C. A.; Taylor, M. S. *J. Am. Chem. Soc.* **2011**, *133*, 10559.
(46) Zierkiewicz, W.; Wieczorek, R.; Hobza, P.; Michalska, D. *Phys. Chem. Chem. Phys.* **2011**, *13*, 5105.
(47) Walter, S. M.; Kniep, F.; Herdtweck, E.; Huber, S. M. *Angew. Chem., Int. Ed.* **2011**, *50*, 7187.
(48) Rosenfield, R. E.; Parthasarathy, R.; Dunitz, J. D. *J. Am. Chem. Soc.* **1977**, *99*, 4860.
(49) Burling, F. T.; Goldstein, B. M. *J. Am. Chem. Soc.* **1992**, *114*, 2313.
(50) Nagao, Y.; Hirata, T.; Goto, S.; Sano, S.; Kakehi, A.; Iizuka, K.; Shiro, M. *J. Am. Chem. Soc.* **1998**, *120*, 3104.
(51) Iwaoka, M.; Takemoto, S.; Tomoda, S. *J. Am. Chem. Soc.* **2002**, *124*, 10613.
(52) Werz, D. B.; Gleiter, R.; Rominger, F. *J. Am. Chem. Soc.* **2002**, *124*, 10638.
(53) Bleiholder, C.; Werz, D. B.; Koppel, H.; Gleiter, R. *J. Am. Chem. Soc.* **2006**, *128*, 2666.
(54) Aakeröy, C. B.; Fasulo, M.; Schultheiss, N.; Desper, J.; Moore, C. *J. Am. Chem. Soc.* **2007**, *129*, 13772.
(55) Choudhary, A.; Gandla, D.; Krow, G. R.; Raines, R. T. *J. Am. Chem. Soc.* **2009**, *131*, 7244.
(56) Jakobsche, C. E.; Choudhary, A.; Miller, S. J.; Raines, R. T. *J. Am. Chem. Soc.* **2010**, *132*, 6651.
(57) Vener, M. V.; Egorova, A. N.; Tsirelson, V. G. *Chem. Phys. Lett.* **2010**, *500*, 272.
(58) Wang, W.; Xin, J.; Zhang, Y.; Wang, W.; Lu, Y. *Int. J. Quantum Chem.* **2011**, *111*, 644.
(59) Junming, L.; Yunxiang, L.; Subin, Y.; Weiliang, Z. *Struct. Chem.* **2011**, *22*, 757.
(60) Solimannejad, M.; Gharabaghi, M.; Scheiner, S. *J. Chem. Phys.* **2011**, *134*, 024312.
(61) Scheiner, S. *J. Chem. Phys.* **2011**, *134*, 094315.
(62) Scheiner, S. *J. Chem. Phys.* **2011**, *134*, 164313.
(63) Scheiner, S. *J. Phys. Chem. A* **2011**, 115, DOI: 10.1021/jp203964b.
(64) Scheiner, S. *Chem. Phys. Lett.* **2011**, *514*, 32.
(65) Scheiner, S. *Chem. Phys.* **2011**, *387*, 79.
(66) Frisch, M. J.; Trucks, G. W.; Schlegel, H. B.; Scuseria, G. E.; Robb, M. A.; Cheeseman, J. R.; Zakrzewski, V. G.; Montgomery, J. A.Jr.; Stratmann, R. E.; Burant, J. C.; Dapprich, S.; Millam, J. M.; Daniels, A. D.; Kudin, K. N.; Strain, M. C.; Farkas, O.; Tomasi, J.; Barone, V.; Cossi, M.; Cammi, R.; Mennucci, B.; Pomelli, C.; Adamo, C.; Clifford, S.; Ochterski, J.; Petersson, G. A.; Ayala, P. Y.; Cui, Q.; Morokuma, K.; Malick, D. K.; Rabuck, A. D.; Raghavachari, K.; Foresman, J. B.; Cioslowski, J.; Ortiz, J. V.; Baboul, A. G.; Stefanov, B. B.; Liu, G.; Liashenko, A.; Piskorz, P.; Komaromi, I.; Gomperts, R.; Martin, R. L.; Fox, D. J.; Keith, T.; Al-Laham, M. A.; Peng, C. Y.; Nanayakkara, A.; Gonzalez, C.; Challacombe, M.; Gill, P. M. W.; Johnson, B.; Chen, W.; Wong, M. W.; Andres, J. L.; Gonzalez, C.; Head-Gordon, M.; Replogle, E. S.; Pople, J. A. *Gaussian 03*; D.01 ed.; Gaussian, Inc.: Pittsburgh, PA, 2003.
(67) Hermida-Ramón, J. M.; Cabaleiro-Lago, E. M.; Rodríguez-Otero, J. *J. Chem. Phys.* **2005**, *122*, 204315.
(68) Riley, K. E.; Op't Holt, B. T.; Merz, K. M. J. *J. Chem. Theory Comput.* **2007**, *3*, 407.
(69) Lu, Y.-X.; Zou, J.-W.; Fan, J.-C.; Zhao, W.-N.; Jiang, Y.-J.; Yu, Q.-S. *J. Comput. Chem.* **2008**, *30*, 725.
(70) Hyla-Kryspin, I.; Haufe, G.; Grimme, S. *Chem. Phys.* **2008**, *346*, 224.
(71) Biswal, H. S.; Wategaonkar, S. *J. Phys. Chem. A* **2009**, *113*, 12774.
(72) Osuna, R. M.; Hernández, V.; Navarrete, J. T. L.; D'Oria, E.; Novoa, J. J. *Theor. Chem. Acc.* **2011**, *128*, 541.
(73) Zeng, Y.; Zhang, X.; Li, X.; Zheng, S.; Meng, L. *Int. J. Quantum Chem.* **2011**, *111*, 3725.
(74) Zhao, Q.; Feng, D.; Sun, Y.; Hao, J.; Cai, Z. *Int. J. Quantum Chem.* **2011**, *111*, 3881.
(75) Hauchecorne, D.; Moiana, A.; Veken, B. J. v. d.; Herrebout, W. A. *Phys. Chem. Chem. Phys.* **2011**, *13*, 10204.
(76) Boys, S. F.; Bernardi, F. *Mol. Phys.* **1970**, *19*, 553.
(77) Reed, A. E.; Weinhold, F.; Curtiss, L. A.; Pochatko, D. J. *J. Chem. Phys.* **1986**, *84*, 5687.
(78) Reed, A. E.; Curtiss, L. A.; Weinhold, F. *Chem. Rev.* **1988**, *88*, 899.
(79) Szalewicz, K.; Jeziorski, B. Symmetry-Adapted Perturbation Theory of Intermolecular Interactions. In *Molecular Interactions. From Van der Waals to Strongly Bound Complexes*; Scheiner, S., Ed.; Wiley: New York, 1997; p 3.
(80) Moszynski, R.; Wormer, P. E. S.; Jeziorski, B.; van der Avoird, A. *J. Chem. Phys.* **1995**, *103*, 8058.
(81) Werner, H.-J.; Knowles, P. J.; Manby, F. R.; Schütz, M.; Celani, P.; ; Knizia, G.; Korona, T.; Lindh, R.; Mitrushenkov, A.; Rauhut, G.; Adler, T. B.; Amos, R. D.; Bernhardsson, A.; Berning, A.; Cooper, D. L.; Deegan, M. J. O.; Dobbyn, A. J.; Eckert, F.; Goll, E.; Hampel, C.; Hesselmann, A.; Hetzer, G.; ; Hrenar, T.; Jansen, G.; Köppl, C.; Liu, Y.; Lloyd, A. W.; Mata, R. A.; May, A. J.; McNicholas, S. J.; Meyer, W.; Mura, M. E.; Nicklaß, A.; Palmieri, P.; Pflüger, K.; Pitzer, R.; Reiher, M.; Shiozaki, T.; Stoll, H.; Stone, A. J.; Tarroni, R.; Thorsteinsson, T.; Wang, M.; Wolf, A. *MOLPRO*; Version 2006; 2010.
(82) Cybulski, S. M.; Scheiner, S. *Chem. Phys. Lett.* **1990**, *166*, 57.
(83) Scheiner, S. *Phys. Chem. Chem. Phys.* **2011**, *13*, 13860.
(84) Morokuma, K.; Kitaura, K. Variational approach (SCF ab-initio calculations) to the study of molecular interactions: the origin of molecular interactions. In *Molecular Interactions*; Ratajczak, H., Orville-Thomas, W. J., Eds.; Wiley: New York, 1980; Vol. 1, p 21.
(85) Vanquickenborne, L. G. Quantum chemistry of the hydrogen bond. In *Intermolecular Forces*; Huyskens, P. L., Luck, W. A. P., Zeegers-Huyskens, T., Eds.; Springer-Verlag: Berlin, 1991; p 31.
(86) Sokalski, W. A. *J. Chem. Phys.* **1982**, *77*, 4529.
(87) Gu, Y.; Kar, T.; Scheiner, S. *J. Am. Chem. Soc.* **1999**, *121*, 9411.
(88) Morokuma, K. *Acc. Chem. Res.* **1977**, *10*, 294.
(89) Scheiner, S.; Kar, T. *J. Phys. Chem. A* **2002**, *106*, 1784.
(90) Mo, Y.; Bao, P.; Gao, J. *Phys. Chem. Chem. Phys.* **2011**, *13*, 6760.
(91) Zhao, Q.; Feng, D.; Sun, Y.; Hao, J.; Cai, Z. *J. Mol. Model.* **2011**, *17*, 1935.
(92) Zahn, S.; Frank, R.; Hey-Hawkins, E.; Kirchner, B. *Chem.—Eur. J.* **2011**, *22*, 6034.
(93) Romaniello, P.; Lelj, F. *J. Phys. Chem. A* **2002**, *106*, 9114.
(94) Wang, W.; Tian, A.; Wong, N.-B. *J. Phys. Chem. A* **2005**, *109*, 8035.
(95) Alkorta, I.; Blanco, F.; Solimannejad, M.; Elguero, J. *J. Phys. Chem. A* **2008**, *112*, 10856.
(96) Amezaga, N. J. M.; Pamies, S. C.; Peruchena, N. M.; Sosa, G. L. *J. Phys. Chem. A* **2010**, *114*, 552.
(97) Iwaoka, M.; Komatsu, H.; Katsuda, T.; Tomoda, S. *J. Am. Chem. Soc.* **2004**, *126*, 5309.
(98) Bleiholder, C.; Gleiter, R.; Werz, D. B.; Köppel, H. *Inorg. Chem.* **2007**, *46*, 2249.
(99) Gleiter, R.; Werz, D. B.; Rausch, B. J. *Chem.—Eur. J.* **2006**, *9*, 2676–2683.
(100) Hayashi, S.; Nakanishi, W.; Furuta, A.; Drabowicz, J.; Sasamori, T.; Tokitoh, N. *New J. Chem.* **2009**, *33*, 196.
(101) Sarma, B. K.; Mugesh, G. *ChemPhysChem* **2009**, *10*, 3013.
(102) Pal, T. K.; Sankararamakrishnan, R. *J. Phys. Chem. B* **2010**, *114*, 1038–1049.
(103) Lu, Y.-X.; Zou, J.-W.; Wang, Y.-H.; Jiang, Y.-J.; Yu, Q.-S. *J. Phys. Chem. A* **2007**, *111*, 10781.

(104) Crestani, M. G.; Manbeck, G. F.; Brennessel, W. W.; McCormick, T. M.; Eisenberg, R. *Inorg. Chem.* **2011**, *50*, 7172–7188.
(105) Hu, J.; Nguyen, M.-H.; Yip, J. H. K. *Inorg. Chem.* **2011**, *50*, 7429–7439.
(106) Platel, R. H.; White, A. J. P.; Williams, C. K. *Inorg. Chem.* **2011**, *50*, 7718–7728.
(107) Helm, M. L.; Stewart, M. P.; Bullock, R. M.; DuBois, M. R.; DuBois, D. L. *Science* **2011**, *333*, 863.